Available online at www.sciencedirect.com
SCIENCE DIRECT®
Journal of Solid State Chemistry 178 (2005) 22–27
JOURNAL OF SOLID STATE CHEMISTRY
www.elsevier.com/locate/jssc

A combined X-ray and neutron Rietveld study of the chemically lithiated electrode materials $Li_{2.7}V_3O_8$ and $Li_{4.8}V_3O_8$

S. Jouanneau, A. Verbaere*, D. Guyomard

Laboratoire de Chimie des Solides, Institut des Matériaux Jean Rouxel, 2, rue de la Houssinière, BP 32229, 44322 Nantes Cedex 03, France

Received 30 August 2004; received in revised form 4 October 2004; accepted 6 October 2004

Abstract

The lithium insertion in the positive electrode material $Li_{1+\alpha}V_3O_8$ (α close to 0.1–0.2) includes a phenomenon near 2.6 V (voltage vs. the Li metal electrode), the mechanism being a two-phase process with the transformation from ca. $Li_{2.9}V_3O_8$ to ca. $Li_4V_3O_8$. Near 2.4 V down to 2 V, Li is inserted in a single phase up to ca. $Li_5V_3O_8$. Chemical Li insertions have been performed in a $Li_{1.1}V_3O_8$ precursor prepared at 350 °C and the structures of the products $Li_{2.7}V_3O_8$ (before the 2.6 V phenomenon) and $Li_{4.8}V_3O_8$ (near the expected maximum) have been studied by a combined Rietveld refinement of X-ray and neutron diffraction data. The structure of $Li_{4.8}V_3O_8$ is an ordered derivative of the rock-salt type, with all the Li and V ions in slightly distorted octahedral sites. $Li_{2.7}V_3O_8$ has a poor crystallization state and, although the expected V_3O_8 layers are obtained, only a part of the Li sites have been reliably determined. Between adjacent V_3O_8 layers, several unidentified sites are likely weakly occupied, thus giving a markedly disordered character for the structure of the compound formed just before the transition at 2.6 V. The atomic shifts at the transition are briefly discussed.
© 2004 Elsevier Inc. All rights reserved.

Keywords: Vanadium oxide; Lithium vanadate; Hewettite; Structure; Lithium insertion; Lithium battery

1. Introduction

$Li_{1+\alpha}V_3O_8$ is a non-stoichiometric bronze obtained for α close to 0.1–0.2 [1,2]. It is an attractive starting material for practical applications in a positive electrode of rechargeable lithium battery, as, in the voltage range 3.7–2.0 V, the samples prepared at a moderate temperature can reversibly insert more than 3 Li atoms per formula unit [2–10]. (In the present paper, all the voltages are given vs. a Li metal electrode.)

The crystal structure of $Li_{1+\alpha}V_3O_8$, first determined by Wadsley [11], was further refined by Picciotto et al. [12]. It is a member of the hewettite group [13], with a layered structure, which results from the stacking of V_3O_8 anionic layers held together by Li ions (Fig. 1). A V_3O_8 layer is formed by chains of VO_6 distorted octahedra and VO_5 distorted square pyramids connected to each other by corner and/or edge sharing. Per formula unit, 1 Li resides in an octahedral site (site fully occupied, labelled "Li(1)"), and α Li are in a tetrahedral site. After Ref. [12], the latter site is the one labelled "Li(2)" in Fig. 1, and its refined site occupancy factor (SOF) is 0.10(5). Another author, using neutron diffraction, did not confirm the occupancy of this site (a slightly negative SOF is reported for Li(2) in Ref. [2]) and supposed that the α Li are spread over several of the other possible tetrahedral sites [2,11,12].

Previous powder X-ray diffraction (XRD) experiments have shown that the chemical or electrochemical insertion of Li occurs into two phases $Li_{1+x}V_3O_8$: from $x = \alpha$ to $x \approx 1.9$, Li is inserted in the single phase $Li_{1+\alpha}V_3O_8$ (voltage domain 3.7–2.65 V); and from $x \approx 3$ to $x \approx 4$, Li is inserted in the single phase $Li_4V_3O_8$ (voltage domain 2.5–2 V). In between, the mechanism is a two-phase process with the transformation from

*Corresponding author. Fax: +33 2 40 37 39 95.
E-mail address: verbaere@cnrs-imn.fr (A. Verbaere).

0022-4596/$ - see front matter © 2004 Elsevier Inc. All rights reserved.
doi:10.1016/j.jssc.2004.10.009

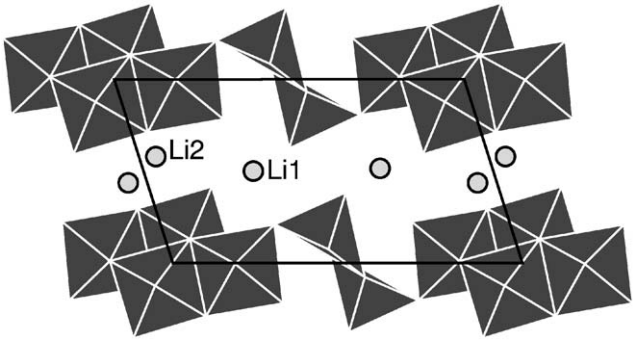

Fig. 1. [010] view of the layered structure of $Li_{1+\alpha}V_3O_8$ (space group $P2_1/m$; $\alpha \approx 0.2$; the c-axis is horizontal, within a V_3O_8 layer). A layer is formed of chains of distorted VO_6 and VO_5 polyhedra running parallel to the b-axis. The circles represent the octahedral site Li(1) and the tetrahedral site Li(2), between the layers [11,12].

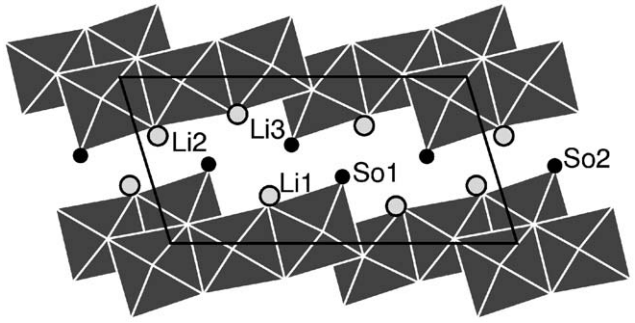

Fig. 2. [010] view of the structure of $Li_4V_3O_8$ (space group $P2_1/m$; the c-axis is horizontal, within a V_3O_8 layer). A layer is formed of chains of VO_6 octahedra running parallel to the b-axis. Open circles and dark disks represent the obtained and hypothetical octahedral Li site, respectively [12].

ca. $Li_{2.9}V_3O_8$ to ca. $Li_4V_3O_8$ (voltage near 2.6 V) [2,9,10,12]. Hereafter, the latter transformation is called "Li3–Li4 transition". All the Li insertion phenomena occur with a nearly constant unit-cell volume, the major unit-cell parameter changes being a decrease of parameter a (decrease of the interlayer distance) and an increase of parameter b. The changes are particularly significant at the Li3–Li4 transition [2,9,10,12].

The major features of the crystal structure of $Li_4V_3O_8$ (Fig. 2) have been determined on a chemically lithiated single crystal [12]. It is a defect rock-salt structure, which is derived from its parent $Li_{1+\alpha}V_3O_8$ via unit-cell parameter variations and small atomic displacements. As illustrated by Fig. 2, the coordinations of all the V atoms are octahedral and more symmetrical than in $Li_{1+\alpha}V_3O_8$. Evidence for an octahedral coordination of Li was obtained for 3 of the 4 Li in $Li_4V_3O_8$, so that it was supposed that the Li3–Li4 transition is marked by a change of the sites occupied by Li: from tetrahedral to octahedral sites [12].

To complete the structural knowledge on the mechanisms, chemical Li insertions have been performed in a $Li_{1.1}V_3O_8$ precursor prepared at 350 °C and the structures of the products $Li_{2.7}V_3O_8$ (i.e., before the 2.6 V insertion process) and $Li_{4.8}V_3O_8$ (i.e., near the expected maximum $Li_5V_3O_8$) have been determined by the Rietveld method, using both X-ray and neutron diffraction data. The composition $Li_{2.7}V_3O_8$ has been selected, instead of $Li_{2.9}V_3O_8$, as the latter composition could correspond to a two-phase mixture [9,10].

2. Experimental

The precursor $Li_{1+\alpha}V_3O_8$ ($\alpha = 0.1$) was prepared via a sol–gel route as previously described [2,4], from V_2O_5 in a 1 M $LiOH \cdot H_2O$ aqueous solution for 24 h at 50 °C under N_2. The gel formed was then freeze-dried [6]. The temperature of the final thermal treatment of the solid thus obtained was rather low, 350 °C, to ensure the formation of a finely divided, reactive powder. Samples of $Li_{1.1}V_3O_8$ were lithiated by slowly adding the required amount of a 1.6 M solution of n-butyllithium in hexane to a suspension of 500 mg of the solid in 50 ml of hexane, and by stirring the suspension for 7 days at 50 °C. The chemical analyses of Li and V by ICP atomic absorption spectroscopy indicate that the reactions of lithiation are practically complete. The relative error on the Li content is 3% approximately.

For the powder XRD, the lithiated samples were placed in SiO_2 capillary tubes sealed under Ar and the patterns were recorded with an INEL system, for 15 h, using Cu$K\alpha_1$ radiation. The powder neutron diffraction data were collected for 24 h (2θ from 3° to 170°; step of 0.1°; $\lambda = 2.3433$ Å) at the G4.2 diffractometer of the Laboratoire Léon Brillouin, Saclay, France. The multipattern Rietveld refinements were performed using the GSAS software package [14]. The background was fitted by fixing 15–25 background points. For the first refinements, the starting atomic positions were those given [12] for $Li_{1+\alpha}V_3O_8$ or $Li_4V_3O_8$ in the space group $P2_1/m$. Geometric and crystal chemical considerations as well as Fourier and Fourier difference syntheses gave information on the possible positions of the remaining Li atoms. The site occupancy factor (SOF) of each of these Li positions was systematically refined, by first fixing arbitrarily the isotropic thermal parameter U_{iso} and the fractional atomic co-ordinates xyz. For $Li_{2.7}V_3O_8$, in many cases it was not possible to simultaneously refine the SOF, xyz, and U_{iso} for Li, and these parameters were refined in turn. In the case of the Li(1) and Li(2) sites in $Li_{2.7}V_3O_8$, although significant SOF were obtained, it was not possible to refine the Li location and obtaining acceptable Li–O distances. For these atoms, the locations have been fixed near the center of the site, at the point indicated by the

Fourier syntheses. After many refinements including individual isotropic and/or anisotropic thermal parameters, overall parameters U_{iso} were refined for each atomic species in the last refinements.

3. Results and discussion

A few lithiated samples $Li_{1+x}V_3O_8$ have been prepared, with compositions in the range $1<x<4$. They have been studied by powder XRD and the results of the unit-cell parameter refinements agree with the general variations of parameters previously reported by Kawakita et al. [9,10]. However, note that in Refs. [9,10] two phases are observed in the range $1.5<x<3.2$, while for $x=1.7$ we obtained a single phase (i.e. before the Li3–Li4 transition). In the same manner, for a starting compound $Li_{1+\alpha}V_3O_8$ prepared at higher temperature, Picciotto et al. obtained a single phase at $x=3$ (i.e. after the Li3–Li4 transition) [12]. Thus, the compositions of the two phases present in the mixtures during the Li3–Li4 transition are not known with precision.

Figs. 3 and 4 illustrate the differences in the crystallinities of $Li_{2.7}V_3O_8$ and $Li_{4.8}V_3O_8$. For $Li_{2.7}V_3O_8$, all the lines in the XRD pattern are much broader than for the precursor and no line is truly distinguished for $2\theta>67^\circ$. For refinements, the angular range of the X-ray pattern was thus restrained to $2\theta<90^\circ$. For $Li_{4.8}V_3O_8$, the line broadening is clearly less and XRD lines are visible after $2\theta\approx80^\circ$. This result is unexpected, as $Li_{4.8}V_3O_8$ is heavily lithiated and it is situated after the Li3–Li4 transition. In the neutron diffraction patterns, the line width is less sensitive to the crystallinity, which is mainly due to the apparatus.

3.1. Structure of $Li_{2.7}V_3O_8$

The structure still results from the stacking of V_3O_8 layers held together by Li. Fig. 5(a) illustrates the result of the first refinement, which concerned the layers V_3O_8 and the octahedral sites Li(1). Globally, the structure of

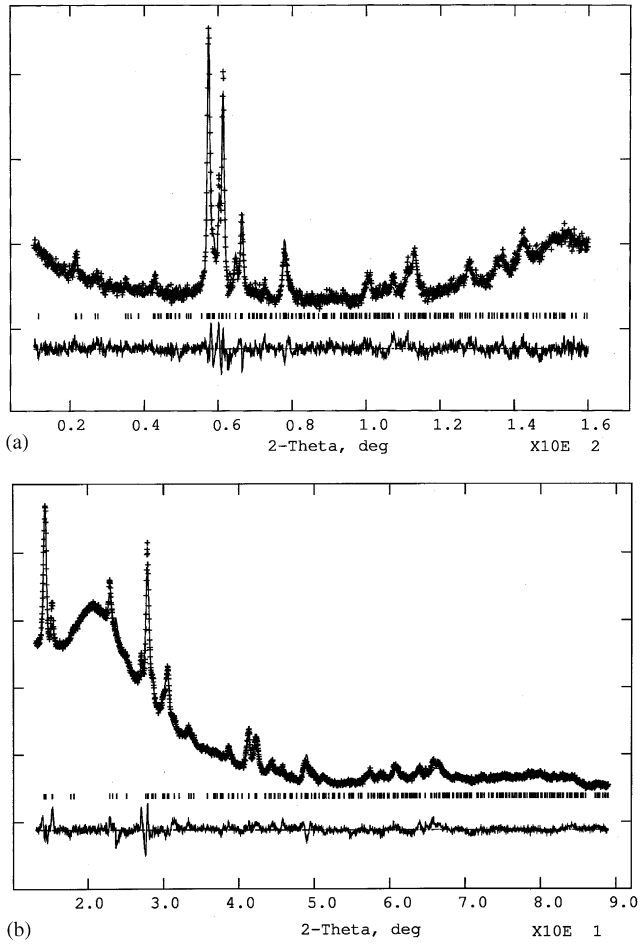

Fig. 3. Rietveld refinement plot of $Li_{2.7}V_3O_8$ with observed (+) and calculated (−) profiles, and difference on the same scale. The line positions are marked by bars. (a) Neutrons data, and (b) X-ray data.

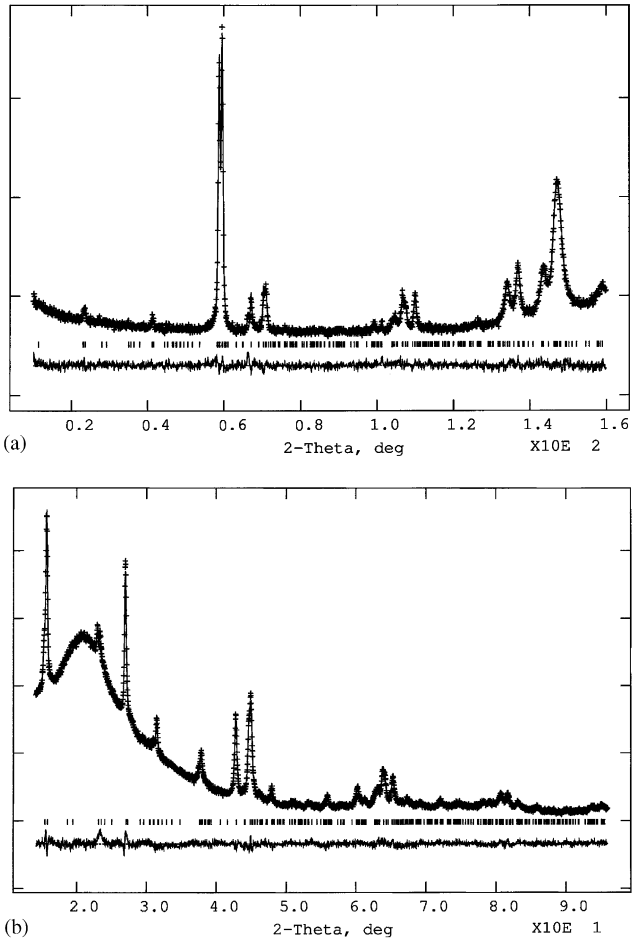

Fig. 4. Rietveld refinement plot of $Li_{4.8}V_3O_8$ with observed (+) and calculated (−) profiles, and difference on the same scale. The line positions are marked by bars. (a) Neutrons data, and (b) X-ray data.

this part (V_3O_8 and Li(1)) is roughly the same as that in Fig. 1, with however a smaller parameter *a* (which governs the interlayer distance). Fig. 5(a) also indicates the regions where acceptable sites are found for Li in the structure. Apart from Li(1), they are tetrahedral sites. Fig. 5(a) and (b), however, clearly show that they correspond to octahedral sites, as well, when the next nearest neighbors are included in the environments. The double character (tetrahedral and octahedral) of the tetrahedral Li sites was already remarked [12] in the parent $Li_{1+\alpha}V_3O_8$. Note that all the Li polyhedra involved are far from regular.

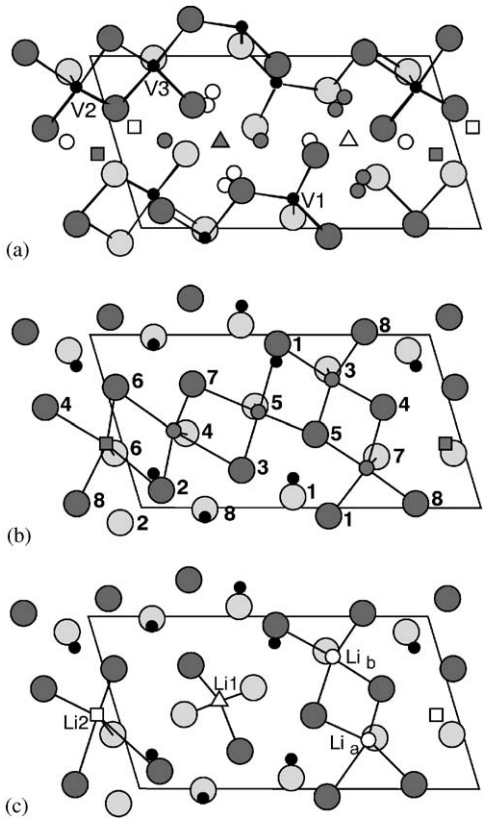

Fig. 5. [010] view of the structure of $Li_{2.7}V_3O_8$ (space group $P2_1/m$; the *c*-axis is horizontal, within a V_3O_8 layer). Large circles represent oxygen atoms at $y=\frac{1}{4}$ (open circles) or $\frac{3}{4}$. Dark disks represent V atoms at $y=\frac{1}{4}$ or $\frac{3}{4}$. (a) Squares (Li(2)), small circles and triangles (Li(1)) represent possible Li sites at $y=\frac{1}{4}$ (light) or $\frac{3}{4}$ (gray) between two adjacent V_3O_8 layers. (b) Squares and small circles represent possible regions of octahedral Li sites (see the text; equivalent sites are not shown, for clarity); the label number of the oxygen atoms is indicated. (c) Squares, small circles and triangles show the sites occupied by Li, owing to the refinement results (equivalent occupied sites are not shown, for clarity).

Tables 1–3 and Fig. 3 summarize the results, and Fig. 5(c) shows the Li sites which appear to be significantly occupied. Globally, despite the refinement conditions being various and numerous, the quality of the results is less than that usually reported for Rietveld refinements, for the following reasons:

- Several remaining peaks in the difference profiles of Fig. 3 reveal the remaining problems of peak intensity (see also the *R* factors in Table 1).
- Indeed the expected V_3O_8 layers are obtained. However, one of the V–O bond lengths (1.58(4) for V(2)–O(6)) is shorter than that expected considering

Table 2
Fractional atomic coordinates, site occupancy factors (SOF) and isotropic thermal parameters U_{iso} for $Li_{2.7}V_3O_8$; space group $P2_1/m$

Atom	*x/a*	*y/b*	*z/c*	SOF	U_{iso} (Å^2)
V(1)	0.838(7)	1/4	0.527(4)	1	1.3(4)
V(2)	0.189(5)	1/4	0.066(3)	1	1.3(4)
V(3)	0.060(8)	1/4	0.820(4)	1	1.3(4)
O(1)	0.055(4)	1/4	0.4555(22)	1	2.70(11)
O(2)	0.904(4)	1/4	0.9247(22)	1	2.70(11)
O(3)	0.792(4)	1/4	0.6719(22)	1	2.70(11)
O(4)	0.426(3)	1/4	0.1969(23)	1	2.70(11)
O(5)	0.581(4)	1/4	0.4233(26)	1	2.70(11)
O(6)	0.307(4)	1/4	0.9685(24)	1	2.70(11)
O(7)	0.289(3)	1/4	0.7399(22)	1	2.70(11)
O(8)	0.985(4)	1/4	0.1869(28)	1	2.70(11)
Li(1)	0.508	1/4	0.696	0.69(8)	2.70(11)
Li(a)	0.722(8)	1/4	0.281(5)	1.00(10)	3.5
Li(b)	0.24(3)	1/4	0.315(18)	0.32(11)	3.5
Li(2)	0.58	1/4	0.05	0.20(10)	3.5

U_{iso} is multiplied by 100.

Table 1
Crystal data and conditions for the last refinement

Compound	$Li_{2.7}V_3O_8$		$Li_{4.8}V_3O_8$	
Unit-cell parameters	$a=6.438(2)$ Å	$b=3.722(1)$ Å	$a=5.9177(3)$ Å	$b=4.0283(2)$ Å
	$c=12.149(4)$ Å	$\beta=106.72(2)^\circ$	$c=12.1154(6)$ Å	$\beta=106.543(4)^\circ$
	Volume = 278.8 Å^3		Volume = 277.2 Å^3	
Data	X-ray	Neutron	X-ray	Neutron
R_{exp} (%)	2.31	3.31	1.47	3.11
R_{wp} (%)	6.58	3.77	5.82	2.88
R_p (%)	1.61	2.83	1.40	2.30
R_F (%)/number of *hkl*	31.0/278	12.4/223	11.6/305	10.7/207
R_{F2} (%)/number of *hkl*	24.1/264	9.5/214	14.5/320	7.48/218

Table 3
Selected interatomic distances (Å) in $Li_{2.7}V_3O_8$

V(1)–O(1)	1.85(3)	V(1)–O(1)	1.98(9)	V(1)–O(1)	1.98(9)
V(1)–O(3)	1.86(4)	V(1)–O(5)	1.77(4)		
V(2)–O(2)	2.12(3)	V(2)–O(2)	1.969(8)	V(2)–O(2)	1.969(8)
V(2)–O(4)	1.86(4)	V(2)–O(6)	1.58(4)	V(2)–O(8)	2.23(5)
V(3)–O(2)	1.83(3)	V(3)–O(3)	2.11(3)	V(3)–O(6)	2.03(4)
V(3)–O(7)	1.99(4)	V(3)–O(8)	1.882(4)	V(3)–O(8)	1.882(4)
Li(1)–O(3)	1.93	Li(1)–O(4)	2.24	Li(1)–O(4)	2.24
Li(1)–O(5)	2.33	Li(1)–O(5)	2.33	Li(1)–O(7)	1.64
Li(a)–O(1)	2.55(6)	Li(a)–O(4)	1.88(5)	Li(a)–O(5)	2.17(7)
Li(a)–O(7)	1.877(8)	Li(a)–O(7)	1.877(8)	Li(a)–O(8)	2.30(7)
Li(b)–O(1)	2.33(20)	Li(b)–O(3)	1.88(3)	Li(b)–O(3)	1.88(3)
Li(b)–O(4)	2.13(21)	Li(b)–O(5)	2.22(20)	Li(b)–O(8)	1.90(20)
Li(2)–O(4)	2.28	Li(2)–O(6)	1.75	Li(2)–O(6)	2.03
Li(2)–O(6)	2.03	Li(2)–O(8)	2.66		

Table 4
Fractional atomic coordinates, site occupancy factors (SOF) and isotropic thermal parameters U_{iso} for $Li_{4.8}V_3O_8$; space group $P2_1/m$

Atom	x/a	y/b	z/c	SOF	U_{iso} (Å^2)
V(1)	0.865(5)	1/4	0.553(3)	1	0.73(24)
V(2)	0.177 (4)	1/4	0.0699(26)	1	0.73(24)
V(3)	0.019(6)	1/4	0.817(3)	1	0.73(24)
O(1)	0.120(5)	1/4	0.4412(27)	1	0.65(10)
O(2)	0.836(5)	1/4	0.933(3)	1	0.65(10)
O(3)	0.752(5)	1/4	0.685(3)	1	0.65(10)
O(4)	0.468(5)	1/4	0.185(3)	1	0.65(10)
O(5)	0.606(5)	1/4	0.438(4)	1	0.65(10)
O(6)	0.316(5)	1/4	0.945(3)	1	0.65(10)
O(7)	0.179(5)	1/4	0.688(3)	1	0.65(10)
O(8)	0.014(5)	1/4	0.179(3)	1	0.65(10)
Li(1)	0.262(12)	1/4	0.302(8)	1	2.1(3)
Li(2)	0.659(18)	1/4	0.063(11)	1	2.1(3)
Li(3)	0.773(12)	1/4	0.321(8)	1	2.1(3)
Li(4)	0.429(19)	1/4	0.557(10)	0.77(7)	2.1(3)
Li(5)	0.542(17)	1/4	0.813(11)	1	2.1(3)

U_{iso} is multiplied by 100.

the V–O bonding scheme, even when the large standard deviation is taken into account.

- The site occupancies correspond to 2.2 Li, instead of 2.7 Li, per formula unit.

As there is no evidence for any extra phase in the samples, and as the unit-cell parameters fairly agree with the chemical composition, we suppose that the above problems are mainly due to the crystallinity and to a disordered situation for Li between the layers. The Li(a) site being fully occupied, 1.7 Li are distributed over at least three sites, and likely five sites or regions (Fig. 5(a) and (b)), since the missing ca. 0.5 Li is likely distributed over the other tetrahedral sites.

The site Li(1), which is fully occupied in the precursor, is still significantly occupied, although it is poorly adapted to Li, in the mean structure, after the decrease in the interlayer distance upon Li insertion. One must suppose that, where the Li(1) site is occupied, the local structure is significantly distorted to better accommodate Li. The same is true, probably, for other Li sites.

3.2. Structure of $Li_{4.8}V_3O_8$

Evidence for the occupancy of the five octahedral Li sites previously observed or postulated [12] for $Li_4V_3O_8$ was provided by Fourier and Fourier difference mapping. Without any constraint, the values of the Li SOF refined to ca. 1.1, except that of Li(4) (value of 0.5). The latter SOF refined to 0.77(7), when the other SOF are fixed at 1., thus giving a composition in fair agreement with the chemical analyses. Tables 1, 4 and 5 and Fig. 4 show that the results are satisfactory.

Figs. 6(a) and 7(a) show representations of the structure, which is in fair agreement with the previous results and hypotheses, and they allow comparisons with $Li_{2.7}V_3O_8$ and $Li_4V_3O_8$. $Li_{4.8}V_3O_8$ has a defect rock salt type structure. On going from $Li_{2.7}V_3O_8$ to $Li_4V_3O_8$ and $Li_{4.8}V_3O_8$, the V and Li polyhedra and environments become more symmetrical. This evolution is easily seen in Figs. 5 and 6, in particular concerning the bonding of V(1), and it accompanies the decrease of the oxidation state of V, which lowers the V–V repulsions. In the same manner, the unit-cell parameters tend to the values which would correspond to them in the case of an ideal cubic symmetry (i.e. a/c, a/b, and β of $2/\sqrt{17}$, $\sqrt{2}$, and 104.04°, respectively). Note that the shortest Li–Li or Li–V distances are Li(4)–Li(4) = 2.7(1) Å and

Table 5
Selected interatomic distances (Å) in $Li_{4..8}V_3O_8$

V(1)–O(1)	2.29(3)	V(1)–O(1)	2.0165(15)	V(1)–O(1)	2.0165(15)
V(1)–O(3)	1.91(4)	V(1)–O(5)	1.75(4)	V(1)–O(7)	2.10(4))
V(2)–O(2)	2.22(3)	V(2)–O(2)	2.0155(12)	V(2)–O(2)	2.0155(12)
V(2)–O(4)	1.88(4)	V(2)–O(6)	1.92(4)	V(2)–O(8)	1.84(3)
V(3)–O(2)	2.00(3)	V(3)–O(3)	1.90(3)	V(3)–O(6)	1.99(3)
V(3)–O(7)	2.04(4)	V(3)–O(8)	2.026(3)	V(3)–O(8)	2.026(3)
Li(1)–O(1)	2.08(9)	Li(1)–O(3)	2.023(8)	Li(1)–O(3)	2.023(8)
Li(1)–O(4)	2.13(8)	Li(1)–O(5)	2.22(9)	Li(1)–O(8)	1.77(9)
Li(2)–O(2)	2.12(10)	Li(2)–O(4)	2.10(10)	Li(2)–O(6)	2.12(12)
Li(2)–O(6)	2.024(9)	Li(2)–O(6)	2.024(9)	Li(2)–O(8)	2.17(13)
Li(3)–O(1)	2.15(9)	Li(3)–O(4)	2.07(9)	Li(3)–O(5)	1.95(8)
Li(3)–O(7)	2.041(12)	Li(3)–O(7)	2.041(12)	Li(3)–O(8)	2.53(9)
Li(4)–O(1)	1.96(12)	Li(4)–O(3)	2.09(12)	Li(4)–O(5)	2.028(12)
Li(4)–O(5)	2.028(12)	Li(4)–O(5)	2.01(9)	Li(4)–O(7)	2.46(10)
Li(5)–O(2)	1.92(12)	Li(5)–O(3)	2.24(10)	Li(5)–O(4)	2.016(4)
Li(5)–O(4)	2.016(4)	Li(5)–O(6)	2.37(12)	Li(5)–O(7)	2.24(12)

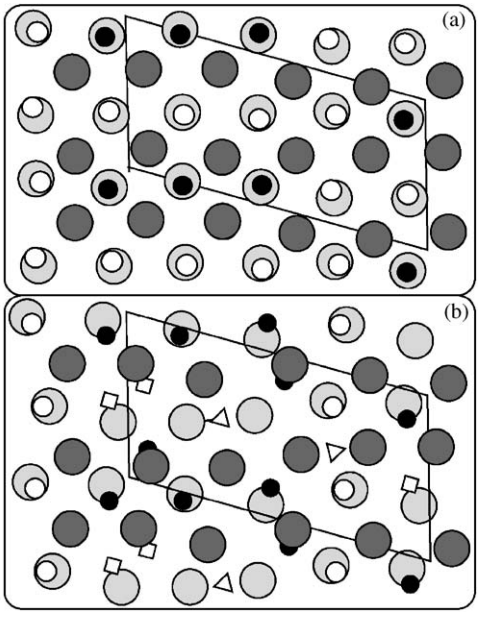

Fig. 6. [010] view of the structure of $Li_{4.8}V_3O_8$ (a) (space group $P2_1/m$; the a-axis is vertical), and comparison with $Li_{2.7}V_3O_8$ (b). Large circles represent oxygen atoms at $y=\frac{1}{4}$ (light) or $\frac{3}{4}$ (darkened). Dark disks represent V atoms at $y=\frac{1}{4}$ or $\frac{3}{4}$. Squares, small circles and triangles represent Li at $y=\frac{1}{4}$ or $\frac{3}{4}$. Several equivalent positions at $y=\frac{1}{4}$ are not visible.

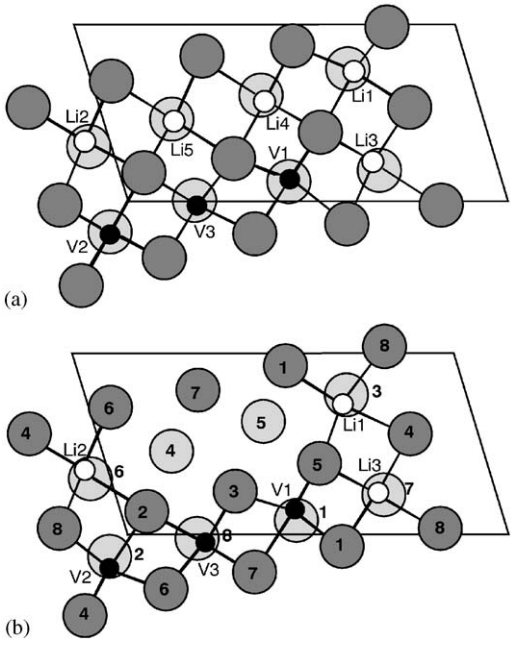

Fig. 7. Detail ([010] view) of the structure of $Li_{4.8}V_3O_8$ (a), comparison with $Li_4V_3O_8$ (b), and indications for the atom labels.

Li(4)–V(1) = 2.6(1) Å; they concern the lithium site Li(4) which do not appear to be fully occupied.

4. Concluding remarks

The Li3–Li4 transition is marked by an increase of parameter b (≈ 0.3 Å) and a decrease of the interlayer distance (≈ 0.4 Å). As illustrated by Fig. 6, the transition does not create supplementary sites for Li (nor an increase of the unit-cell volume), it modifies the features of the Li sites, giving sites better adapted to the crystal chemistry of lithium. Before the transition, apart from the octahedral site Li(1) (triangles in Fig. 6(b), sites which disappear during the transition), all the possible Li sites are intermediate between distorted tetrahedral sites and distorted octahedral sites (see Figs. 5(a) and (b)). After the transition, fairly symmetrical, adapted octahedral sites are available for Li.

Acknowledgments

The authors thank EDF for financial support, and F. Bourée and J. Rodriguez-Carvajal for their help in the Laboratoire Léon Brillouin. S. Jouanneau is also grateful for the research fellowship provided by the DGA.

References

[1] D.G. Wickham, J. Inorg. Nucl. Chem. 27 (1965) 1939.
[2] S. Jouanneau, Ph.D. Thesis: Nantes, 2001.
[3] G. Pistoia, M. Pasquali, M. Tocci, V. Manev, R.V. Moshtev, J. Power Sources 15 (1985) 13.
[4] G. Pistoia, M. Pasquali, G. Wang, L. Li, J. Electrochem. Soc. 137–8 (1990) 2365.
[5] J. Kawakita, Y. Katayama, T. Muria, T. Kishi, Mat. Res. Soc. Symp. Proc. 496 (1998) 391.
[6] K. West, B. Zachau-Christiansen, S. Skaarup, M.Y. Saidi, J. Barker, I.I. Olsen, R. Pynenburg, R. Koksbang, J. Electrochem. Soc. 143 (1996) 820.
[7] J. Kawakita, Y. Katayama, T. Muria, T. Kishi, Solid State Ionics 110 (1998) 199.
[8] M.Y. Saidi, I.I. Olsen, R. Koksbang, J. Barker, R. Pynenburg, K. West, B. Zachau-Christiansen, Mat. Res. Symp. Proc. Ser. 369 (1995) 201.
[9] J. Kawakita, T. Muria, T. Kishi, Solid State Ionics 118 (1999) 141.
[10] J. Kawakita, T. Muria, T. Kishi, Solid State Ionics 120 (1999) 109.
[11] A.D. Wadsley, Acta Crystallogr. 10 (1957) 261–267.
[12] L.A. de Picciotto, K.T. Adendorff, D.C. Liles, M.M. Thackeray, Solid State Ionics 62 (1993) 297–307.
[13] H.T. Evans, J.M. Hughes, Am. Mineral. 75 (1990) 508–521.
[14] A.C. Larson, R.B. von Dreele, Generalized Structure Analysis System, University of California, Los Alamos, 1994.